TAMPERE UNIVERSITY OF TECHNOLOGY

Mikko Poikkimäki

SOA formation yields in atmosphere

Updated: 14.8.2013

TABLE OF CONTENTS

1. INTRODUCTION

2. THEORY

2.1 Diffusion in binary mixtures

Diffusion illustrates mass convection in medium from greater consentration to lower consentration. Fick's law states diffusion flux

$$J = -D_{AB}\frac{dn}{dx}, \tag{2.1}$$

where D_{AB} is binary diffusion coefficient and n molecule number consentration.

Diffusion coefficient for binary gasmixtures can be calculated from Reid et al. (1987)

$$D_{AB} = 0.001 \cdot T^{1.75}\frac{\sqrt{\frac{1}{M_A}+\frac{1}{M_B}}}{p(V_A^{1/3}+V_B^{1/3})^2}, \tag{2.2}$$

where unit of diffusion coefficient is cm^2/s, temperature T is Kelvin, molar masses M are g/mol and pressure p is bar. Diffusion volumes V can be calculated from values for atomic diffusion volumes which are for carbon C 15.9, for hydrogen 2.31, for oxygen 6.11, for nitrogen 4.54, for heterocyclic ring -18.3 and for air 19.7.

Diffusion related vapor mean free path according to Pirjola and Kulmala (1998)

$$\lambda = \frac{3D_{AB}}{\bar{c}_A}, \tag{2.3}$$

where $\bar{c}_A$ is velocity of gas molecules

$$\bar{c}_A = \sqrt{\frac{8RT}{\pi M_A}}, \tag{2.4}$$

where R is ideal gas constant 8.31446 J/Kmol.

For example $C_{10}H_{16}O_{10}$ molecule ($M_A \approx 300$) with one heterocyclic ring, diffusion volume $V_A \approx 250$. Diffusion coefficient of this molecule in air in temperature 290 K and pressure 1 atm is 0.0489 cm^2/s. Related mean free path λ is 102.65 nm.

2.2 Condensation sink

Condensation sink represents rate how rapidly condensable vapor molecules condenses on existing aerosol in units 1/s. It can be calculated from

$$CS = 2\pi D \int_0^\infty d_p \beta(d_p) n(d_p)\,\mathrm{d}d_p = 2\pi D \sum_i \beta d_{pi} N_i, \tag{2.5}$$

where d_{pi} is the diameter of a particle in size class i, N_i is corresbonding particle number consentration (Dal Maso et al., 2002) and D is diffusion coefficient of condensing vapor. Transition regime correction factor β_m according to Fuchs and Sutugin (1971) is

$$\beta_m = \frac{1+Kn}{1+\left(\frac{4}{3\alpha_m}+0.337\right)Kn+\frac{4}{3\alpha_m}Kn^2} \tag{2.6}$$

where α_m is the sticking coefficient which represents probability of molecule to stick in to the particle. Dimensioless Knudsen number is

$$Kn = \frac{2\lambda}{d_p}, \tag{2.7}$$

where λ is the effective mean free path of the condensing vapor molecules in the gas. Knudsen number is the ratio of two lenght scales. Mean free path λ characterizes the gas with respect to the transport of mass and particle diameter d_p characterizes the droplet.

One can semiempirically represent condensation sink as a function of aerosol mass as follows

$$CS = 2 \cdot 10^{-4} \cdot N^{0.37} M^{0.63}, \tag{2.8}$$

where N is particle number and M particle mass.

2.3 Proposed chemical reaction of monoterpene, SLLV source

Monoterpene reaction with ozone and hydroxyl produces SLLV product with molecular yield of α and other products with mass yields of β_i

$$\mathrm{MT+O_3+OH} \xrightarrow{\mathrm{k}} \alpha \mathrm{C_{vap}} + \textstyle\sum_i \beta_i \mathrm{C_i} \tag{2.9}$$

Source of SLLV vapor is then

$$Q_{vap} = \alpha k P, \tag{2.10}$$

where P is precursor (monoterpene) consentration and overall reaction rate $k = k_{O_3}[\mathrm{O_3}] + k_{OH}[\mathrm{OH}]$ is reaction rate of ozone times ozone consentration plus reaaction rate of hydroxyl times hydroxyl consentration.

Proposed SLLV product sinks

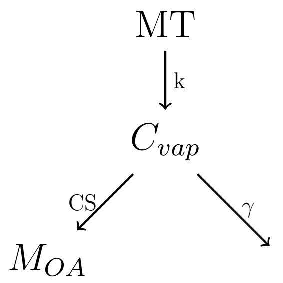

Figure 2.1: Proposed routes for monoterpene precursor MT reaction (rate k) SLLV product C_{vap}. To aerosol M_{OA} with rate CS or to walls or other losses with rate γ

2.4 Hydroxyl radical concentration diurnal variation in atmosphere

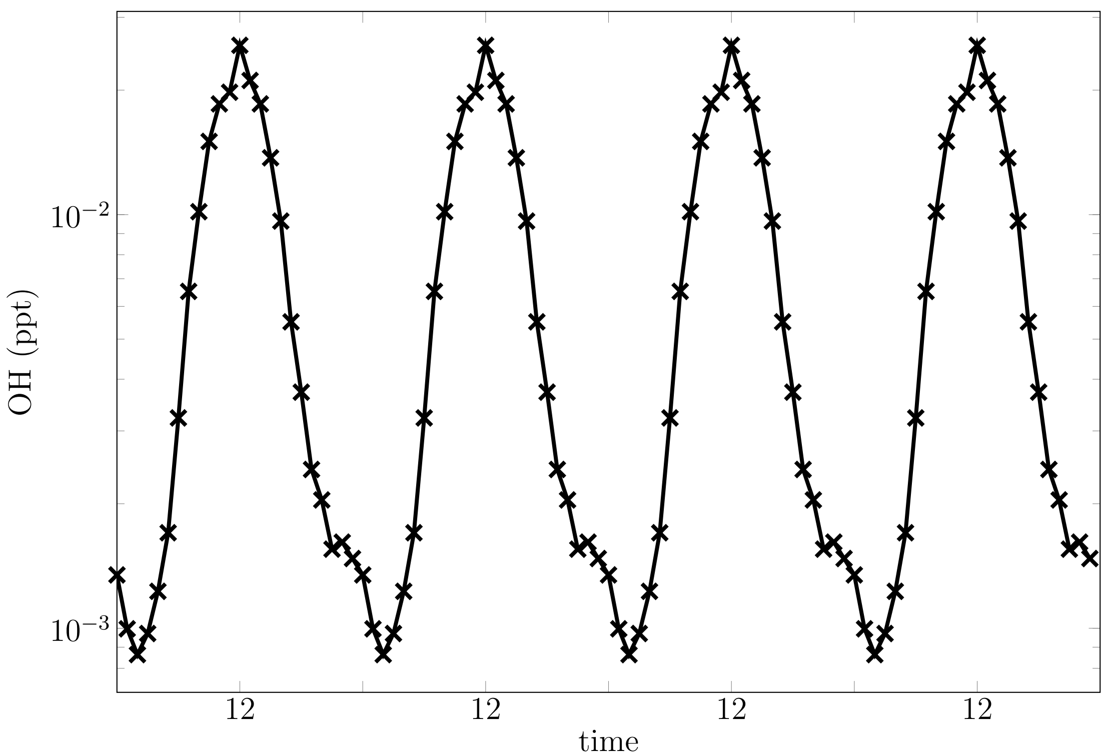

Figure 2.2: Diurnal variation of hydroxyl radical median concentration measured in spring and summer 2007 in Hyytiälä on new particle formation event days. Hourly datapoints (crosses) are from Petäjä et al. 2009 and solid line is used in modelling. Time is from midnight to midnight and noons are marked.

2.5 Ozone concentration diurnal variation in atmosphere

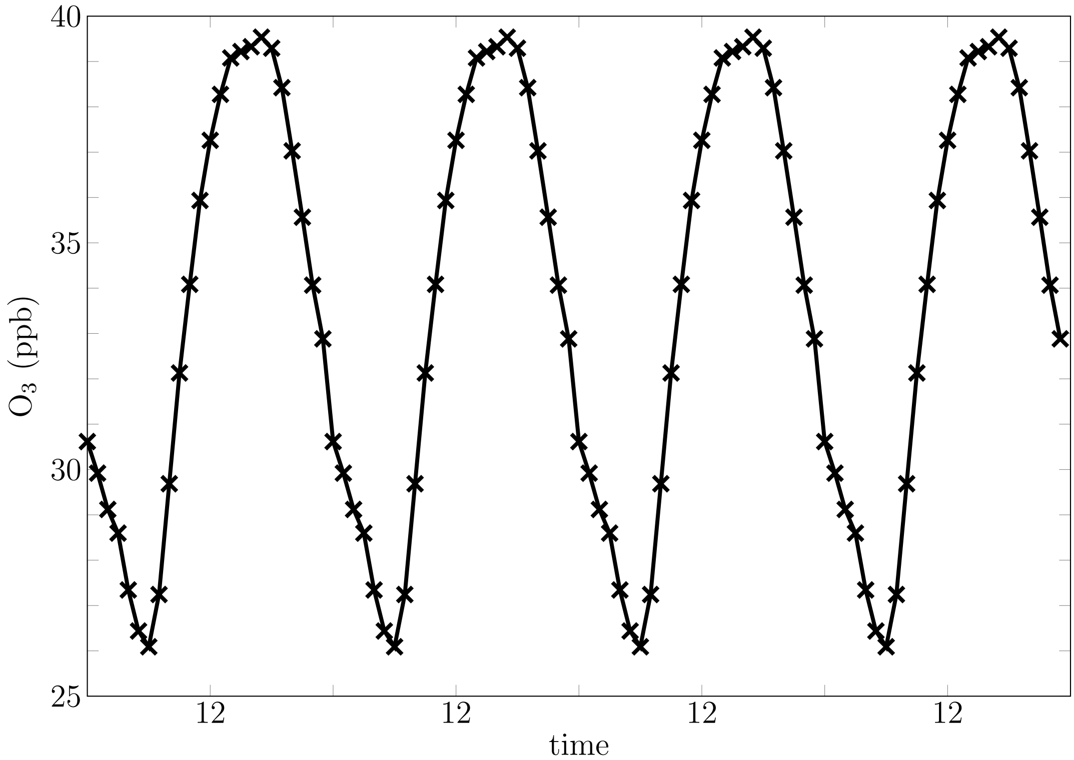

Figure 2.3: Diurnal variation of mean ozone concentration measured summertime in 1997-2003 in Hyytiälä on new particle formation event days. Hourly datapoints (crosses) are from Lyubovtseva et al. 2005 and solid line is used in modelling.

2.6 Diurnal variation of atmospheric temperature

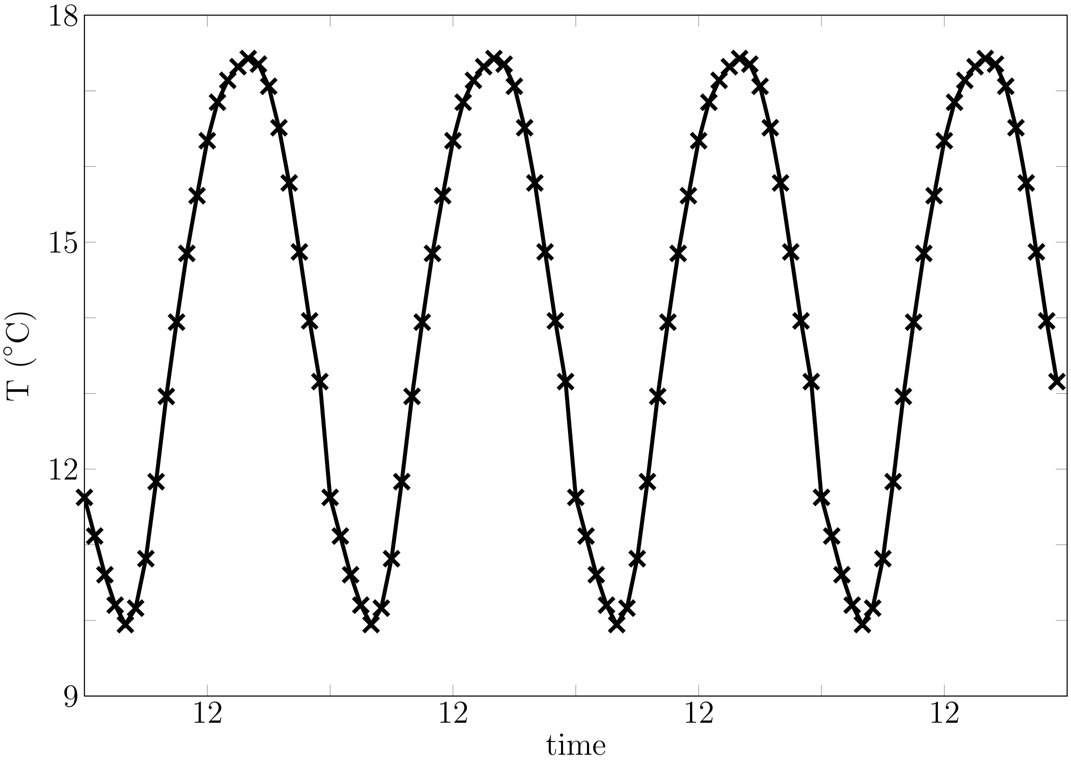

Figure 2.4: Diurnal variation of mean temperature measured summertime in 1997-2003 in Hyytiälä on new particle formation event days. Hourly datapoints (crosses) are from Lyubovtseva et al. 2005 and solid line is used in modelling.

This temperature variation is used in monoterpene emission modelling.

2.7 Diurnal variation of monoterpene emissions

The temperature dependence of the monoterpene emission is described by Guenther et al. (1993)

$$E = E_{30} exp[\beta(T - 30°C)], \tag{2.11}$$

where E is the emission, E_{30} is the normalized emission potential and β is the temperature dependence coefficient. Commonly used value for β is 0.09°C^{-1} and emission potential value 1.37 mg/m^{2}h (Rinne et al., 2007) was used to obtain diurnal variation of monoterpene emissions presented in figure 2.5. Emission unit milligrams per squaremetre of land per hour was trasformed to concentration per second (cm^{-3}s^{-1}) considering atmospheric box 1000mx1mx1m = 1000m^3 with height 1km.

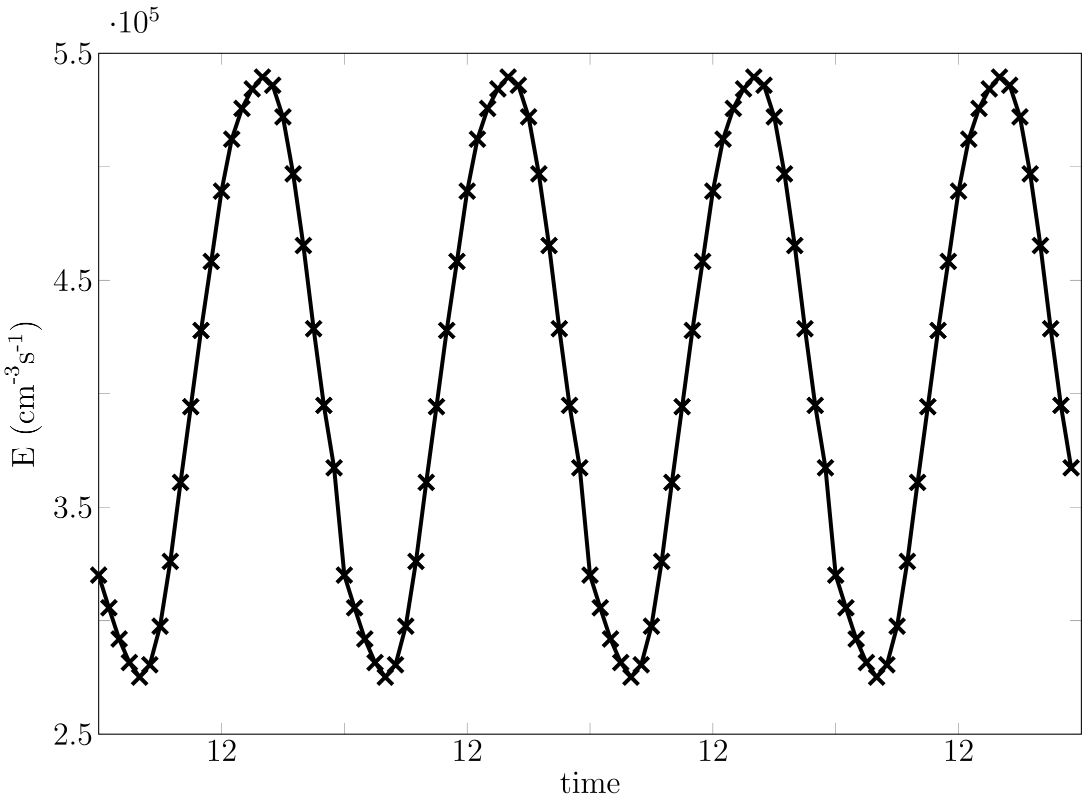

Figure 2.5: Diurnal variation of monoterpene emissions using G93 model. Hourly datapoints (crosses) are calculated from G93 and solid line is used in modelling.

3. METHODS

Particle size distribution varies in time through different processes as nucleation, condensation, coagulation, sedimentation and dilution. These changes can be modelled with general dynamic equation (GDE) (Seinfeld and Pandis, 1998)

$$\frac{\partial n(v,t)}{\partial t} = \frac{1}{2}\int_0^v \mathrm{K}(v-q,q)n(v-q,t)\,\mathrm{d}q - n(v,t)\int_0^\infty \mathrm{K}(q,v)n(q,t)\,\mathrm{d}q$$
$$-\frac{\partial}{\partial v}[I(v)n(v,t)] + J_0\delta(v-v_0) + S(v) - R(v), \qquad (3.1)$$

where I is particle volume changing rate, J_0 is nucleation rate, K is coagulation coefficient, n is size distribution function, R particle loss rate, S particle sources emission rate, t is time, v and $q = v + dv$ are particle volumes and $\delta(v - v_0)$ is Dirac's delta function which is one whenever $v = v_0$ and otherwise zero. Two first term of equation represents coagulation, third term condensation, fourth nucleation, fifth other particle sources and the last other particle sinks like deposition.

3.1 Used sectional aerosol model

In sectional model particle size distribution is divided in desired amount of size sections which are characterized with two parametres: particle size and consentration. Particle population is considered monodispersive in each section. In this study moving center model was used where section borders are fixed but particle sizes can vary inside sections (Korhonen, 2004). Model takes into account particle coagulation, dilution and nucleation, vapor condensation in to the particles, vapor dilution and loss to walls (or other places).

Coagulation is modelled with parts of discrete general dymanic equation (Seinfeld and Pandis, 1998)

$$\frac{dN_k}{dt} = \frac{1}{2}\sum_{j=g^*}^{k-g^*} K_{j,k-j}N_jN_{k-j} - N_k\sum_{j=g^*}^{\infty} K_{k,j}N_j, \qquad (3.2)$$

where first term represents increase of particles in section k and second term reduction of particles through coagulation.

Condensation growth of particles is modelled by growing section size using growth rate (Seinfeld and Pandis, 1998)

$$\frac{dd_p}{dt} = \frac{2M_{vap}I}{\pi\rho d_p^2 N_A}, \tag{3.3}$$

where M_{vap} is condensing vapor molecular mass, ρ particle density, N_A Avogadro's number and I flux of molecules to the particle phase. It is obtained from

$$I = 2\pi d_p D C_{vap} \beta_m, \tag{3.4}$$

where D is diffusion coefficient, C_{vap} consentration of condensing vapor and β_m obtained from equation 2.6.

Dilution of particle consentration is modelled with equation

$$\frac{dN_k}{dt} = -\gamma_{dil} N_k, \tag{3.5}$$

where γ_{dil} is dilution coefficient in units 1/s. It is inverse value of aerosol lifetime τ.

Used condensing vapor consentration gradient

$$\frac{dC_{vap}}{dt} = Q - CS \cdot C_{vap} - \gamma C_{vap} - \gamma_{dil} C_{vap}, \tag{3.6}$$

takes into account vapor source rate Q, vapor loss rate to particles CS and to walls γ and vapor dilution rate γ_{dil}.

See connection with CS and I

$$CS = \sum_i I_i N_i. \tag{3.7}$$

This is connection between particle growth and vapor loss to particles. These differential equations 3.2, 3.3,3.5 and 3.6 are solved numerically using Runge-Kutta-method (Dormand and Prince, 1980) and time evolution of number distribution function dN/dd_p is gained among other results.

3.2 Used monoterpene reaction model

Monoterpene precursor consentration P was modelled using differential equation

$$\frac{dP}{dt} = E - k_{OH}[OH] \cdot P - k_{O_3}[O_3] \cdot P. \tag{3.8}$$

This monoterpene consentration varies through chemical reaction 2.9 and biogenic emissions E.

3.3 How models was used

In this study batch type aerosol chamber was modelled with 60 size sections between sizes 1 nm and 1 µm. Different aerosol mass seeds M_0 and monoterpene consentrations P_0 was used for two particle sizes and two SLLV wall loss coefficient resulting 4x4x2x2 = 64 model runs. Used constants and variables are presented in table 3.1.

Table 3.1: Used values in modelling. Those values kept same in each model run are presented first and then values that changed between are under.

Constant	Symbol	Unit	Value
Stoichiometric yield of SLLV	α	-	0.08
Sticking coefficient	α_m	-	1
Dilution coefficient	γ_{dil}	1/s	$5\cdot 10^{-5}$
SLLV wall loss coefficient	γ	1/s	$5\cdot 10^{-5}$
SLLV vapor mean free path	λ	nm	102.65
Particle density	ρ	g/cm^3	1.4
Geometric mean deviation GMD	σ	-	1.6
Diffusion coefficient of SLLV	D_{AB}	cm^2/s	0.0489
Reaction rate of ozone	k_{O_3}	cm^3s^{-1}	$9\cdot 10^{-17}$
Reaction rate of hydroxyl	k_{OH}	cm^3s^{-1}	$5\cdot 10^{-11}$
Molar mass of SLLV	M_{vap}	g/mol	300
Molar mass of monoterpene	M_{MT}	g/mol	137
Pressure	p	atm	1
Temperature	T	K	290
Time vector	t	hours	0 - 95

Variable	Symbol	Unit	Value
Count median diameter CMD	μ	nm	80
Background number consentration	N	$1/cm^3$	500
Initial monoterpene consentration	P_0	ppb	10, 50, 100, 200
Ozone consentration	$[0_3]$	ppb	60

Nucleation was modelled with nucleation rate J of 3 nm particles presented in figure 3.1. Nucleation starting at 11:00 and ending at 14:00.

Conversion of ppb to $1/cm^3$ is done multipling with $p/kT = 2.5331\cdot 10^{19}$ air molecules/cm^3.

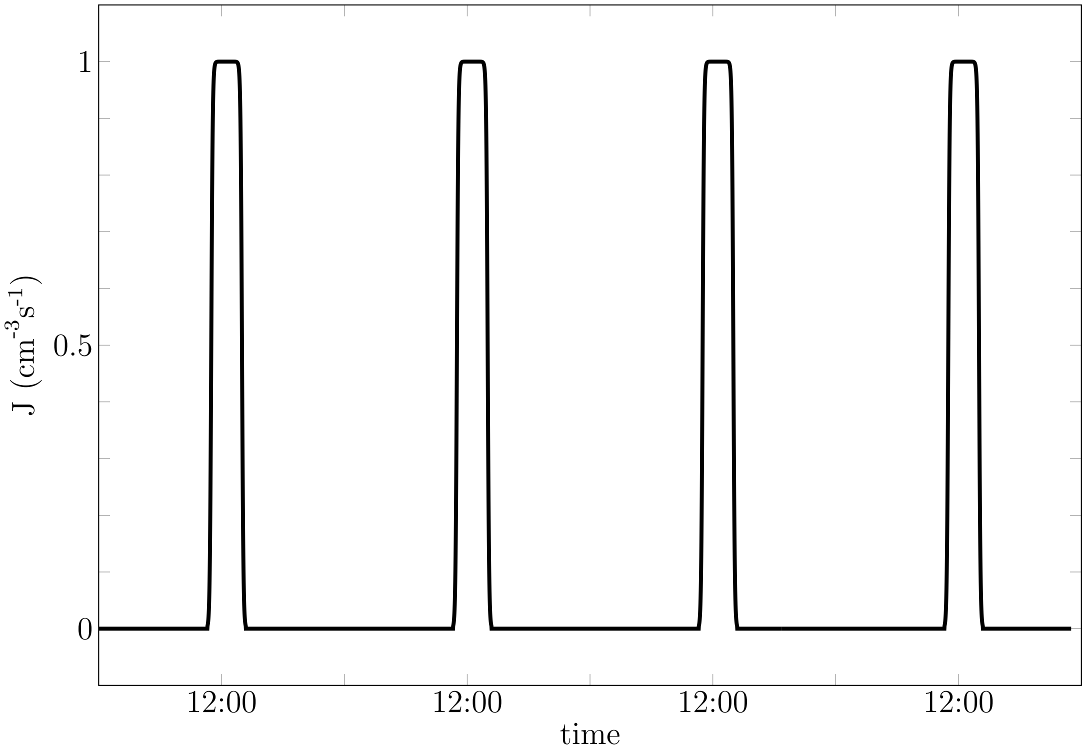

Figure 3.1: 3 nm sized particle nucleation rate used in modelling

3.4 Analysing tools for results, how to get α and γ?

Aerosol mass yield

$$Y = \frac{\Delta M}{\Delta P}, \tag{3.9}$$

where ΔM is formed aerosol mass and ΔP is used precursor mass. Formed aerosol mass can be calculated

$$\Delta M = M_{tot} - M_0 + M_{dil}, \tag{3.10}$$

where M_{tot} is aerosol total mass, M_0 initial aerosol mass and M_{dil} diluted aerosol mass. From particle number distribution dN/dd_p, total aerosol number N_{tot}, volume V_{tot} and mass M_{tot} is integrated considering spherical particles with density $\rho = 1.4$ g/cm^3. Diluted aerosol number N_{dil} is calculated by model from differential equation 3.5. From N_{dil} diluted mass M_{dil} can be calculated and formed aerosol mass got.

Used precursor ΔP is calculated from

$$\Delta P = \int_0^{t_{end}} kP \, \mathrm{d}t, \tag{3.11}$$

where t_{end} is elapsed time, k is formation rate and P is precursor consentration presented in equation 2.10.

Condensation sink was calculated from equation 2.5 using particle number distribution dN/dd_p and values of table 3.1.

Proposed relation for yield and condensation sink

$$Y_{end} = \frac{\alpha}{1 + \frac{\gamma}{CS_{end}}}. \tag{3.12}$$

Using equation 2.8, this relation can be presented as function of aerosol mass

$$Y_{end} = \frac{\alpha}{1 + \frac{\gamma}{2 \cdot 10^{-4} \cdot N^{0.37} M^{0.63}}}. \tag{3.13}$$

Fitting these functions to yield data results knowledge of stoichiometric coefficient of SLLV product α and chamber wall losses γ.

4. RESULTS

4.1 Monoterpene consentration modelling

Solution of differential equation 3.8 (figure 4.1) using diurnal atmospheric values presented in chapter 2 is used to produce source Q_{vap} for condensing vapour using

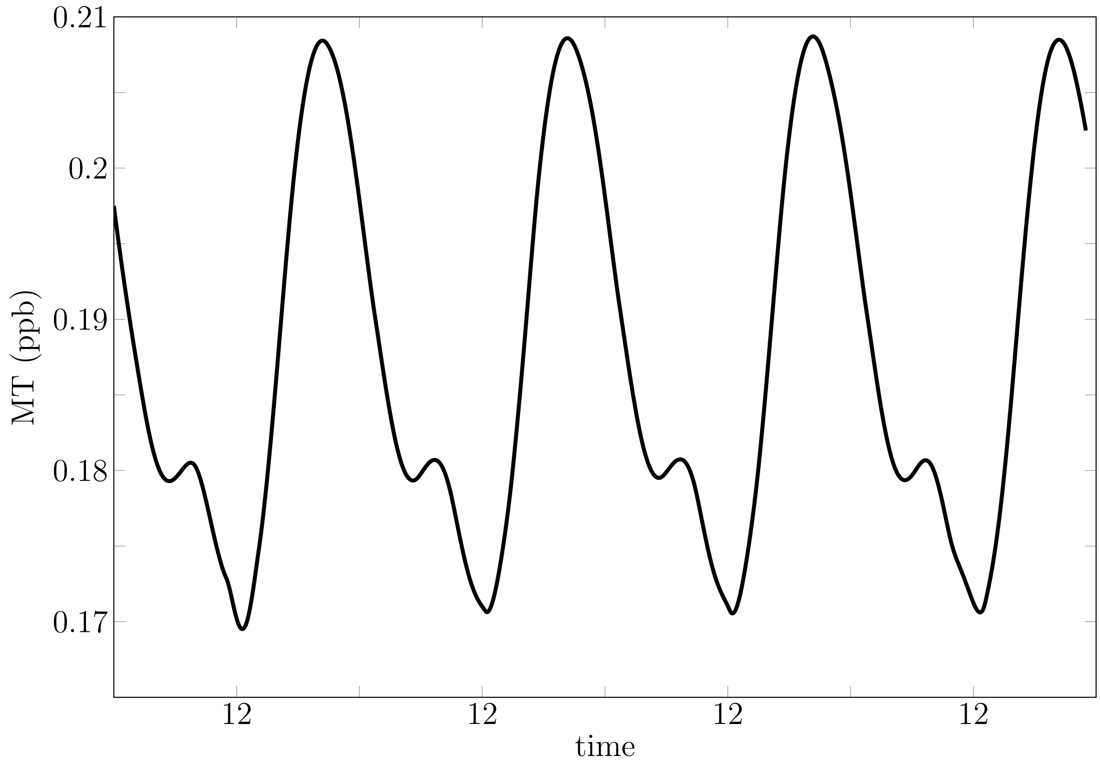

Figure 4.1: Diurnal variation of monoterpene consentration.

equation 2.10.

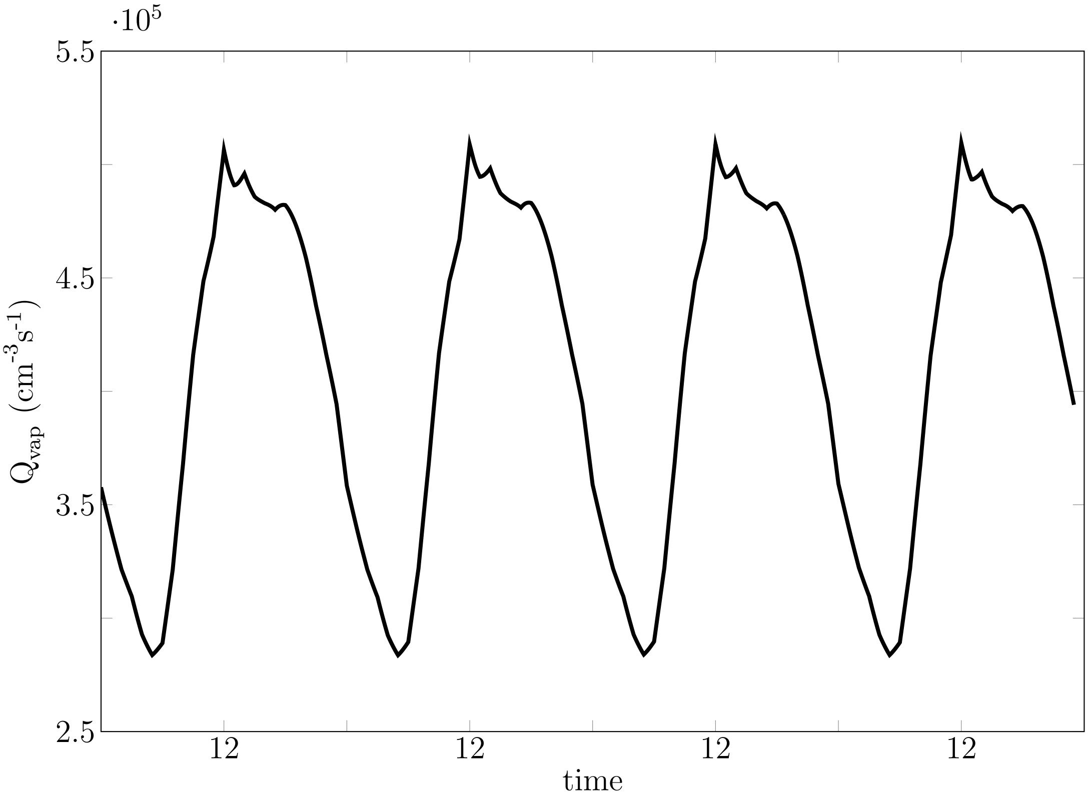

Figure 4.2: Diurnal variation of monoterpene consentration.

4.2 Atmospheric SOA formation modelling

5. CONCLUSION

Matlab scripts and data files to get figure 5.1:
\GitHub\AECHAMO\calculate and plot\Many_subplots_atm.m
and \GitHub\AECHAMO\gaskinetics_mp\MT_kinetics_night_and_day.m
and \GitHub\AECHAMO\Results and scripts_mp\SOA formation\ATM modelling\v4\run_20130814T114856.mat
and \GitHub\AECHAMO\gaskinetics_mp\o3_OH_MT_T_Variable_values.m

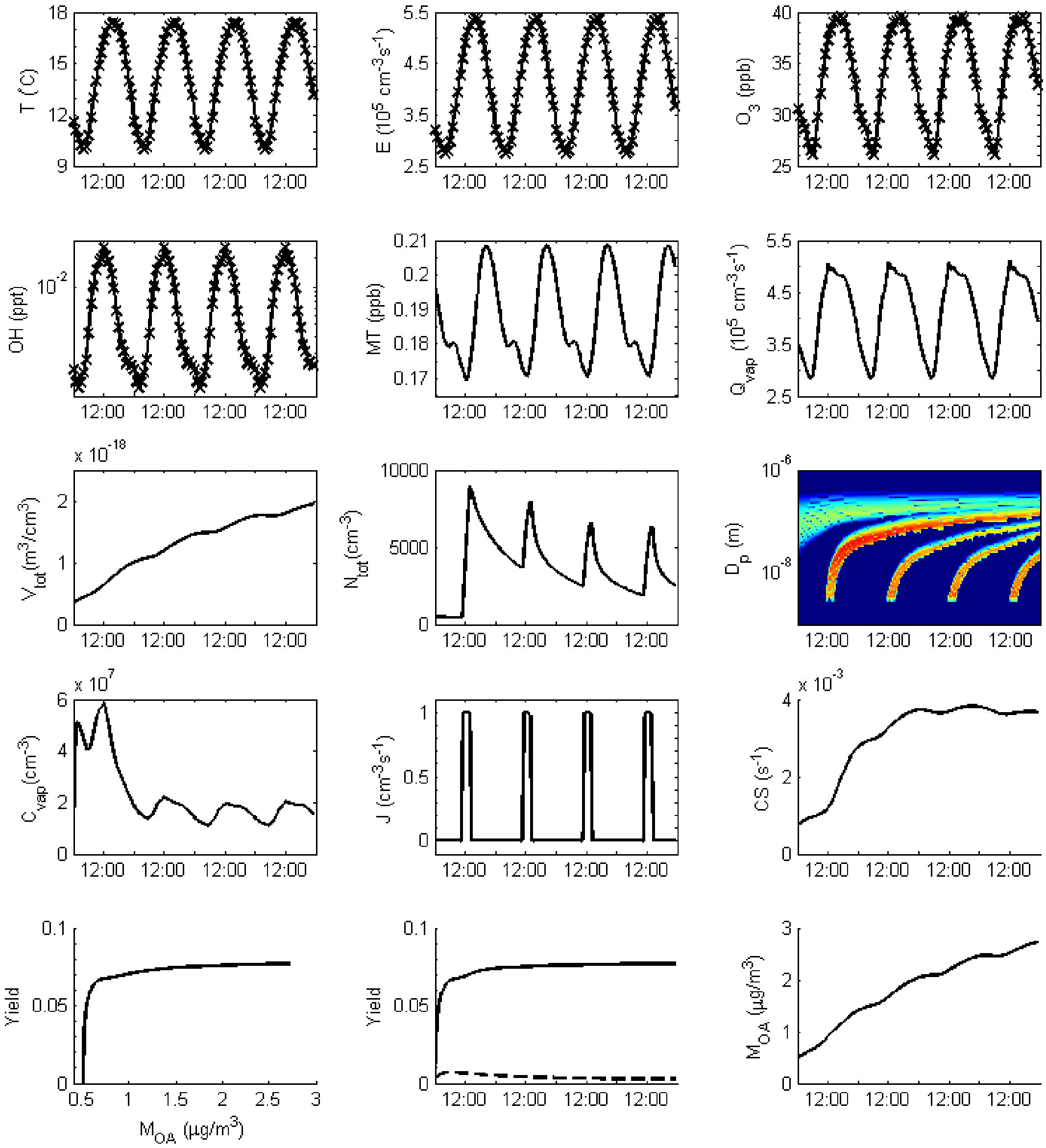

Figure 5.1: All parametres during four day modelling.

REFERENCES

Dal Maso, M., Kulmala, M., Lehtinen, K. E. J., Mäkelä, J. M., Aalto, P., and O'Dowd, C. D. (2002). Condensation and coagulation sinks and formation of nucleation mode particles in coastal and boreal forest boundary layers. *Journal of Geophysical Research D: Atmospheres*, 107(19):1–10.

Dormand, J. R. and Prince, P. J. (1980). A family of embedded Runge-Kutta formulae. *Journal of Computational and Applied Mathematics*, 6:19–26.

Guenther, A. B., Zimmerman, P. R., Harley, P. C., Monson, R. K., and Fall, R. (1993). Isoprene and monoterpene emission rate variability: model evaluations and sensitivity analyses. *Journal of Geophysical Research: Atmospheres*, 98(D7):12609–12617.

Korhonen, H. (2004). Model studies on the size distribution dynamics of atmospheric aerosols. *Doctoral thesis. University of Helsinki.*

Lyubovtseva, Y. S., Sogacheva, L., Dal Maso, M., Bonn, B., Keronen, P., and Kulmala, M. (2005). Seasonal variations of trace gases, meteorological parameters, and formation of aerosols in boreal forests. *Boreal environment research*, 10(6):493–510.

Petäjä, T., Mauldin III, R., Kosciuch, E., McGrath, J., Nieminen, T., Paasonen, P., Boy, M., Adamov, A., Kotiaho, T., and Kulmala, M. (2009). Sulfuric acid and oh concentrations in a boreal forest site. *Atmospheric Chemistry and Physics*, 9(19):7435–7448.

Pirjola, L. and Kulmala, M. (1998). Modelling the formation of H_2SO_4-H_2O particles in rural, urban and marine conditions. *Atmospheric Research*, 46(3-4):321–347.

Reid, R., Prausnitz, J., and Poling, B. (1987). *The properties of gases and liquids.* McGraw Hill Book Co., New York.

Rinne, J., Taipale, R., Markkanen, T., Ruuskanen, T., Hellén, H., Kajos, M., Vesala, T., and Kulmala, M. (2007). Hydrocarbon fluxes above a scots pine forest canopy: measurements and modeling. *Atmospheric Chemistry and Physics*, 7(12):3361–3372.

Seinfeld, J. H. and Pandis, S. N. (1998). *Atmospheric Chemistry and Physics - From Air Pollution to Climate Change.* John Wiley & Sons, New York.